The yeast telomerase RNA, TLC1, participates in two distinct modes of TLC1-TLC1 association processes *in vivo*

Tet Matsuguchi, Elizabeth Blackburn

Telomerase core enzyme minimally consists of the telomerase reverse transcriptase domain-containing protein (Est2 in budding yeast *S. cerevisiae*) and telomerase RNA, which contains the template specifying the telomeric repeat sequence synthesized. Here we report that *in vivo*, a fraction of *S. cerevisiae* telomerase RNA (TLC1) molecules form complexes containing at least two molecules of TLC1, via two separable modes: one requiring a sequence in the 3' region of the immature TLC1 precursor and the other requiring Ku and Sir4. Such physical TLC1-TLC1 association peaked in G1 phase and did not require telomere silencing, telomere tethering to the nuclear periphery, telomerase holoenzyme assembly, or detectable Est2-Est2 protein association. These data indicate that TLC1-TLC1 associations reflect processes occurring during telomerase biogenesis; we propose that TLC1-TLC1 associations and subsequent reorganization may be regulatory steps in telomerase enzymatic activation.

1 The Yeast Telomerase RNA, TLC1, Participates in Two Distinct Modes of TLC1-TLC1

2 Association Processes *in vivo*

4 ABSTRACT

5 Telomerase core enzyme minimally consists of the telomerase reverse transcriptase domain-

6 containing protein (Est2 in budding yeast *S. cerevisiae*) and telomerase RNA, which contains the

7 template specifying the telomeric repeat sequence synthesized. Here we report that *in vivo*, a

8 fraction of *S. cerevisiae* telomerase RNA (TLC1) molecules form complexes containing at least

9 two molecules of TLC1, via two separable modes: one requiring a sequence in the 3' region of

10 the immature TLC1 precursor and the other requiring Ku and Sir4. Such physical TLC1-TLC1

11 association peaked in G1 phase and did not require telomere silencing, telomere tethering to the

12 nuclear periphery, telomerase holoenzyme assembly, or detectable Est2-Est2 protein association.

13 These data indicate that TLC1-TLC1 associations reflect processes occurring during telomerase

14 biogenesis; we propose that TLC1-TLC1 associations and subsequent reorganization may be

15 regulatory steps in telomerase enzymatic activation.

17 AUTHORS

18 Tet Matsuguchi

19 Elizabeth H. Blackburn

21 Department of Biophysics and Biochemistry

22 University of California, San Francisco

23 San Francisco, CA

24 United States of America

26 Corresponding Author

27 Elizabeth H. Blackburn

28 600 16th Street Box 2200

29 San Francisco, CA 94158-2517

30 415-476-2824

31 Elizabeth.Blackburn@ucsf.edu

32 INTRODUCTION

34 Telomeric DNA is typically composed of repetitive sequences (TG1-3 repeats in the budding

35 yeast *S. cerevisiae*) that allow recruitment of specialized macromolecular complexes that help

36 replenish and protect telomeres (de Lange, Lundblad & Blackburn, 2006). These include the

37 ribonucleoprotein telomerase, which adds telomeric DNA by the action of its reverse

38 transcriptase-containing subunit (Est2 in *S. cerevisiae*), templated by a sequence within the

39 telomerase RNA component (TLC1 in *S. cerevisiae*), as well as telomere-protective double-

40 stranded and single-stranded telomeric DNA binding proteins, such as Rap1 and Cdc13 in yeast

41 (Jain & Cooper, 2010).

43 Budding yeast telomerase RNA, TLC1, is over 1300 nucleotides in size and, in addition to

44 providing the template for reverse transcription, has extensive secondary structures (Zappulla &

45 Cech, 2004). Certain structures within TLC1 have been defined and form binding sites for Est2

46 and other telomerase factors. The critical central core of TLC1 includes a structurally highly

47 conserved pseudoknot to which Est2 binds, while an Sm-protein binding site is located near the

48 3' end, which is important for the stability and processing of immature TLC1 (Seto et al., 2002;

49 Zappulla & Cech, 2004; Lin et al., 2004; Jiang et al., 2013) (Figure 1A). Previously, it was

50 reported that mutations (*tlc1-42G* and *tlc1-42C*) in a 6-base palindromic sequence, located within

51 the TLC1 precursor 3' region that is cleaved off to form the processed mature TLC1 RNA (see

52 Figure 1A), cause telomeres to be shorter *in vivo* and abrogate dimerization of TLC1 precursor

53 synthesized *in vitro* (Gipson et al., 2007). Additionally, a 48-nucleotide stem motif in TLC1

54 directly binds the Ku70/Ku80 complex, which, in addition to its widely conserved canonical role

55 in non-homologous end joining (NHEJ), is required for many aspects of yeast telomere biology

56 (Stellwagen et al., 2003). This TLC1-Ku interaction, while not absolutely required for telomere

57 maintenance by telomerase *in vivo*, is required for maintenance of full-length telomeres, *in vivo*

58 association of Est2 to telomeres in G1 phase of the cell cycle (Fisher, Taggart & Zakian, 2004),

59 full recruitment of telomeres to the nuclear periphery (Taddei et al., 2004), and transcriptional

60 silencing at telomeres (Boulton & Jackson, 1998). A mutant Ku containing a small insertion,

61 *yku80-135i*, specifically abrogates the TLC1-Ku interaction but leaves NHEJ intact (Stellwagen

62 et al., 2003). Est1 and Est3 are essential factors for telomerase, which together with Est2 and

63   TLC1, make up the telomerase holoenzyme. Est1 associates with the telomerase complex by

64   directly binding to a bulge-stem region of TLC1 conserved in several budding yeasts, and this

65   association is critical for the recruitment of telomerase to telomeres (Seto et al., 2002; Chan,

66   Boulé & Zakian, 2008).

67

68   Human, *S. cerevisiae*, and *Tetrahymena* (ciliated protozoan) telomerases have been inferred to be

69   active as a monomer *in vitro* (Bryan, Goodrich & Cech, 2003; Alves et al., 2008; Shcherbakova

70   et al., 2009; Jiang et al., 2013). However, reports have also suggested that the human, *S.*

71   *cerevisiae*, and *Euplotes* (ciliated protozoan) telomerase complexes can exist in a dimeric (or

72   other oligomeric) forms (Prescott & Blackburn, 1997; Wenz et al., 2001; Beattie et al., 2001;

73   Wang, Dean & Shippen, 2002). Recent single-molecule electron microscopic structural

74   determinations indicate that core human telomerase complex (telomerase RNA, hTER, and

75   reverse transcriptase, hTERT) is a dimer *in vitro* held together by RNA-RNA (hTER-hTER)

76   interaction (Sauerwald et al., 2013).

77

78   Here, we explored possible modes of physical telomerase dimerization *in vivo,* focusing on the

79   yeast telomerase RNA component TLC1. We developed a biochemical method that directly

80   demonstrates a physical TLC1-TLC1 association (dimerization/oligomerization; direct or

81   indirect), quantified in extracts of cells expressing normal amounts of telomerase RNA from the

82   endogenous *TLC1* gene chromosomal locus. We have not determined whether there are more

83   than two molecules of TLC1 that are associated in complexes, so for simplicity, we refer to this

84   as TLC1-TLC1 association. We report here that such TLC1-TLC1 associations occur *in vivo* via

85   two modes, each mode having distinctive requirements. Our evidence supports association

86   between telomerase RNAs occurring during the biogenesis of active telomerase complex, with

87   potential functional importance in the regulation of telomerase activity.

88

89   MATERIALS AND METHODS

90

91   Plasmids

92   The integrating vector, pRS306-TLC1, was provided by Jue Lin. The MS2 CP-binding RNA

93   hairpins were constructed by annealing overlapping oligonucleotide in a standard PCR protocol.

94   The hairpin construct was cloned into the BclI site of pRS306-TLC1. The fusion PCR method

95   was used to construct *tlc1-42G* and *tlc1-42C* alleles, which were cloned between the BclI and

96   XhoI sites of pRS306-TLC1. CEN-ARS versions of the plasmids were made by subcloning

97   BamHI-XhoI fragments of the integrating vectors into the vector pRS316.

98

99   Yeast strains and growth media

100   Yeast strains were in the S288c background and are isogenic with BY4746, except as noted in

101   Table 1 (Baker Brachmann et al., 1998; Tomlin et al., 2001). Yeast cultures were grown in

102   standard rich medium or minimal media (YEPD or CSM). Deletion strains were made using a

103   PCR-based transformation method (Longtine *et al.* 1998). Cell cycle synchronization was

104   achieved by addition of 5 uM alpha-factor for 4 hours, which arrests yeast cells in G1 phase. The

105   cells were released from the arrest by washing away media containing alpha-factor and addition

106   of new media.

107

108   Immunoprecipitation of MS2 hairpin-tagged TLC1

109   TLC1 was tagged with two MS2 coat-protein-binding RNA hairpins at the BclI restriction site in

110   the *TLC1* coding region sequence. This gene construct with its native promoter was integrated at

111   the endogenous chromosomal *TLC1* locus, in tandem with untagged, wild-type *TLC1*, flanking

112   the *URA3* marker. MS2 coat protein fused to 3 Myc epitope tags was expressed either in *tlc1Δ* or

113   in experimental strains containing both tagged and untagged *TLC1*. The MS2 coat protein from

114   tlc1Δ strains were used for coIP experiments using strains yEHB22,807-824. Whole cell lysates

115   were prepared from cultures in log-phase of growth in YEPD (OD$_{600}$=0.6-1.0) using glass beads

116   and bead beaters. The lysis/wash buffer contained 50mM HEPES-KCl pH8.0, 2 mM EDTA, 2

117   mM EGTA, 0.1% Nonidet P40, 10% glycerol, cOmplete EDTA-free protease inhibitors (Roche)

118   and RNasin (Promega; 1 uL / mL). The lysate concentrations were adjusted to A$_{260nm}$ = 40 before

119   immunoprecipitation. For lysates containing co-expressed MS2 coat protein, 400 uL of lysate

120   was mixed with 1.5 mg Dynal ProA magnetic beads (Invitrogen) and 1 ug of monoclonal anti-

121   Myc antibody (9E11, Santa Cruz Biotechnology). For experiments in which MS2 coat protein

122   was purified separately, ProA magnetic beads, anti-Myc antibody, and whole cell lysate

123   containing MS2 coat protein (at A$_{260nm}$=60-80) were incubated for 1-2 hours. The

124   immunoprecipitation was allowed to take place at 4 °C for 4-hours to overnight. The

125 immunoprecipitates were washed 3 times with the wash buffer. For oligonucleotide-directed

126 displacement experiments, the immunoprecipitates on the beads were aliquotted in separate tubes

127 after the first wash. Each sample was subjected to different sets of oligonucleotides diluted to 0.5

128 uM each in the wash buffer and incubated for 1 hour. Further washes were carried out as above

129 before RNA extraction.

130

131 Immunoprecipitation of tagged proteins

132 For immunoprecipitation of tagged proteins (Est2-13xMyc, Est2-3xFLAG), lysates were

133 prepared as described above. For Myc-tagged proteins, the lysate was mixed with 1.5 mg Dynal

134 ProA magnetic beads, and 1 ug 9E11 antibody. For FLAG-tagged proteins, lysate was incubated

135 with 50uL of M2-conjugated agarose beads. For sequential immunoprecipitation of FLAG-

136 tagged proteins followed by Myc-tagged proteins, 15 ug of 3xFLAG peptide was added to the

137 M2-conjugated agarose beads. The eluate was then used for Myc-tag immunoprecipitation as

138 described.

139

140 Quantitative reverse transcription and PCR (qRT-PCR)

141 RNA from input and immunoprecipitates were isolated using RNeasy Mini Kit (Qiagen),

142 including the DNase step as described by the manufacturer. The primer set for PGK1 was

143 designed using IDT's PrimerQuest program. The reverse primers used to distinguish tagged and

144 untagged TLC1 were designed within and at the insertion junction, respectively, of the MS2

145 hairpin tag. One-step reverse transcription and PCR kits were used for all RNA quantifications,

146 except for the quantification of immature TLC1 (Stratagene, Invitrogen). For quantification of

147 immature TLC1, or 3' regions of TLC1, SuperScript III and random hexamer were used for

148 reverse transcription. Subsequently, SYBR Green I Master mix kit (Roche) was used for

149 quantitative PCR. All quantitative PCR runs included serially diluted RNA samples to make

150 standard curve, from which relative quantitative values were derived using the LightCycler

151 software. The oligonucleotide sequences used in qRT-PCR reactions are listed in Table 2.

152

153 Calculation of Fraction TLC1 in Dimer Form

154 Four quantitative values from qRT-PCR assays are used to estimate the fraction of TLC1 in

155 dimer form: untagged and MS2-tagged TLC1 in the input lysate ($TLC1_{IN}$, $MS2_{IN}$), untagged and

156   MS2-tagged TLC1 in MS2-immunoprecipitate ($TLC1_{IP}$, $MS2_{IP}$). The following equations are

157   used:

158   (1) $f(TLC1) = TLC1_{IN} / (TLC1_{IN} + MS2_{IN})$

159   (2) $f(IP) = MS2_{IP} / MS2_{IN}$

160   (3) $n(heterodimer) = TLC1_{IP} / f(IP)$

161   (4) $f(heterodimer) = 2 * f(TLC1) * (1 - f(TLC1))$

162   (5) $n(dimer) = n(heterodimer) / f(heterodimer)$

163   (6) $n(TLC1 \text{ in dimer}) = 2 * n(dimer)$

164   (7) $f(dimer) = n(TLC1 \text{ in dimer}) / (TLC1_{IN} + MS2_{IN})$

165   In the equations above f() represents "fraction of" and n() represents "amount of." (1) Fraction of

166   TLC1 RNAs that are untagged is calculated as the fraction untagged divided by the sum of

167   untagged and MS2-tagged RNAs. (2) Fraction of MS2-tagged TLC1 immunoprecipitated is

168   calculated by dividing the amount of MS2-tagged TLC1 in the precipitate by the amount of

169   MS2-tagged TLC1 in the input lysate. (3) The amount of untagged TLC1 in the precipitate

170   represents untagged TLC1 in the heterodimeric form with the MS2-tagged TLC1. The total

171   amount of heterodimeric TLC1 is estimated by dividing the amount of untagged TLC1 in the

172   precipitate by the fraction of MS2-tagged TLC1 precipitated (Equation 2). (4) The fraction of

173   TLC1 dimers that are in homodimeric (untagged+untagged or MS2-tagged+MS2-tagged) and

174   heterodimeric (untagged+MS2-tagged) are assumed to result from random associations

175   ($f(TLC1)^2$, $f(MS2)^2$, $2 * f(TLC1) * f(MS2)$). Therefore, the fraction of TLC1 dimers in the

176   heterodimeric form is calculated as $2 * f(TLC1) * f(MS2)$ or $2 * f(TLC1) * (1 - f(TLC1))$. (5)

177   The total amount of dimer is calculated by dividing the number of heterodimers (Equation 3) by

178   the fraction of dimers that are heterodimeric (Equation 4). (6) The total amount of TLC1 in

179   calculated by doubling the amount of dimer (Equation 5). (7) Fraction of TLC1 in dimer form is

180   calculated by dividing the amount of TLC1 in dimer form (Equation 6) by the total amount of

181   TLC1 and MS2 in the input lysate.

182

183   Telomere length analysis

184   Genomic DNA was digested with XhoI and separated on a 0.85% agarose gel. DNA was

185   denatured and transferred to a Nylon membrane, and UV-crosslinked with a Stratalinker. The

186   membrane was blotted with telomeric oligonucleotide

187   (5'-CACACCCACACCACACCCACAC-3') labeled with WellRED D3 fluorescent dye at the 5'

188   end. The blotted membrane was scanned and analyzed using the Odyssey Infrared Imaging

189   System (LI-COR). A linear plasmid containing an S. cerevisiae telomeric DNA sequence was

190   included as a marker of size ~500bp.

191

192

193   RESULTS

194   Co-immunoprecipitation assays demonstrate TLC1-TLC1 association *in vivo*

195

196   To quantify the association between different TLC1 molecules in yeast whole-cell extracts, a co-

197   immunoprecipitation (coIP) assay was developed. First, we created a tagged TLC1 RNA for

198   immunoprecipitation using a tandem pair of RNA hairpins that specifically bind to the

199   bacteriophage MS2 Coat Protein. This two-hairpin construct was inserted at one of two sites in

200   regions of TLC1 previously shown to accommodate insertions of modular protein binding

201   domains with minimal if any effect on *in vivo* functions (Bernardi & Spahr, 1972; Zappulla &

202   Cech, 2004) (Figure 1A). Secondly, we fused three copies of myc tag to MS2 Coat Protein and

203   integrated this gene construct into the genome of experimental strains. Co-expression of the MS2

204   hairpin-tagged TLC1 (TLC1-MS2) and myc-tagged Coat Protein (CP-3myc) allowed specific

205   immunoprecipitation of TLC1-MS2 using an anti-myc antibody. Thirdly, we developed

206   quantitative RT-PCR assays to measure levels and recovery of TLC1, using two sets of PCR

207   primers capable of distinguishing and specifically amplifying either the untagged TLC1 or

208   TLC1-MS2 (Figure 2A and 2B).

209   Next, we verified that the insertion of the MS2 tag did not significantly alter TLC1 functions *in*

210   *vivo*. We tested the telomere lengths of strains that have MS2 hairpin insertion at two different

211   sites, nucleotide positions 455 and 1033 of TLC1 (NcoI and BclI sites). The insertion had the

212   least impact at nucleotide position 1033 (Figure 1C), and we used this construct for the rest of

213   the study. The expression level of TLC1-MS2 was comparable to untagged TLC1 (Figure 2C).

214   The association of TLC1-MS2 with Est2 was slightly reduced compared to untagged TLC1,

215   consistent with telomere lengths observed in cells expressing only TLC1-MS2 (Figure 2D).

216

217 Finally, we co-expressed TLC1-MS2 and untagged TLC1 from the endogenous TLC1 locus to

218 test the coIP of untagged TLC1 with TLC1-MS2. As a control, an equal number of cells from

219 two independently cultured strains expressing either only untagged TLC1 or only TLC1-MS2

220 were mixed prior to cell lysis ("Mix" samples in figures). We found that 50-80% of total TLC1-

221 MS2 is immunoprecipitated from lysates made from the co-expression strain and from the mixed

222 population. A significant enrichment of untagged TLC1 in the TLC1-MS2 immunoprecipitate

223 was observed only in the co-expression strain and not in the mixed cell population, indicating

224 that this assay detected bona fide *in vivo* association of separate TLC1 molecules (see Materials

225 and Methods and Figure 2E). After adjusting for the immunoprecipitation efficiency and the fact

226 that this coIP assay only detects heterodimer of TLC1-MS2 and untagged TLC1, we determined

227 that in unsynchronized log phase cell populations, at least 10% of TLC1 is associated with

228 another TLC1 *in vivo* (Figure 2E; see Materials and Methods for calculation). Interestingly, we

229 observed that the fraction of immature TLC1 molecules present in the whole lysate (4-8%)

230 (Mozdy & Cech, 2006) did not significantly change in the immunoprecipitate, indicating that

231 both immature and mature forms of TLC1 participate comparably in TLC1-TLC1 association

232 (Figure 2F).

233

234 The 3' Region of TLC1 is Important for TLC1-TLC1 association

235

236 To determine the regions of TLC1 involved in the TLC1-TLC1 physical association, we

237 designed a nucleic acid competition experiment aimed to disrupt this association by incubating

238 the TLC1 complex(es), extracted as the immunoprecipitates from cell lysates, with excess anti-

239 sense oligonucleotides. We designed 72 overlapping DNA oligonucleotides, each 30 bases in

240 length, that in total were complementary to the full length of the immature TLC1, which includes

241 the 3' region that is cleaved off in the mature form (Figure 1B). These oligonucleotides were

242 incubated with the TLC1-MS2 immunoprecipitate bound to the magnetic beads in the wash

243 buffer (see Materials and Methods). We predicted that the collection of these 72 TLC1 antisense

244 oligos would act as competitors to TLC1-TLC1 association in the immunoprecipitates. As a

245 control, 72 different DNA oligonucleotides designed against other regions of the yeast genome

246 were used. Incubation of the full set of 72 TLC1-antisense oligonucleotides (but not the 72

247 control oligonucleotides) with the immunoprecipitates reduced the amount of untagged TLC1

248   remaining on the affinity beads by about 70%, while not appreciably diminishing the amount of

249   TLC1-MS2 remaining bound to the affinity beads (Figure 3A and B, bottom row). This result

250   indicated that the 72 TLC1-antisense oligonucleotides likely disrupted the association of the

251   untagged TLC1 and TLC1-MS2.

252

253   To further delineate the regions important for the TLC1-TLC1 association, different subsets of

254   oligonucleotides were used in the same experimental set-up. The 72 oligonucleotides were

255   subdivided into intervals encompassing thirds or ninths of the length of the immature TLC1, in

256   order to probe each TLC1 region separately (Figure 3B). The oligonucleotides complementary to

257   the first third (the 5' region) of TLC1 had little effect on disrupting TLC1-TLC1 association,

258   while the oligonucleotides against the central and 3' region intervals had greater effects (Figure

259   3B, Row 2). Even added together, the total of the effects from each of the three separate regions

260   was significantly less than the disruptive effect seen when all 72 oligonucleotides were added

261   simultaneously, suggesting that there is a synergistic effect in adding all oligonucleotides at once.

262   Similarly, separately challenging the TLC1-TLC1 immunoprecipitates in this way with the anti-

263   sense oligonucleotides encompassing each of the one-ninth regions, especially in the 5' regions

264   of TLC1, disrupted the TLC1-TLC1 association to even lesser extents (Figure 3B Row 1).

265

266   Interestingly, TLC1-TLC1 association was disrupted by 30% using the eight antisense

267   oligonucleotides encompassing the TLC1 3' region. Only two of these eight oligonucleotides

268   were complementary to the last 21 bases of the mature form of TLC1; the remaining six

269   oligonucleotides were complementary only to the 3' extension of the un-cleaved, immature form

270   of TLC1 (Figure 1B). As described above, the immature TLC1 molecules accounted for only 4-

271   8% of the total TLC1 signal in the immunoprecipitate (Figure 2F); thus, a reduction solely of

272   immature TLC1 precursors cannot account for the 30% disruption by the 3' most one-ninth

273   TLC1-complementary oligonucleotides. This result suggests that a small region (30 bases)

274   encompassed by just two oligonucleotides had a relatively large effect in disrupting TLC1-TLC1

275   association of the mature form of TLC1.

276

277   Together, these findings indicated that the 3' region of TLC1 transcript is either the most critical

278   for TLC1-TLC1 association to occur *in vivo*, and/or the most vulnerable to subsequent *in vitro*

279 disruption of the associated form. This *in vitro* disruption by the 3' region-targeting

280 oligonucleotides could have been through a direct competition of base-paired regions between

281 two *TLC1* RNAs, through an unwinding of some structural elements of TLC1, or disruption of

282 RNA-protein associations. Additionally, these data suggest that the TLC1-TLC1 association

283 mostly involves tail-tail (*i.e.*, 3'region with 3' region) interactions, rather than head-head (*i.e.*,

284 5'region with 5' region) or head-tail (*i.e.*, 5'region with 3' region) formations.

285

286 Prompted by the importance of the 3' region of TLC1, we tested the potential role in TLC1-

287 TLC1 association for a previously identified, palindromic sequence located in the 3' region

288 cleaved off during TLC1 maturation and thus present only in the immature, precursor TLC1

289 molecules. This palindromic sequence is evolutionarily conserved among budding yeast species

290 (Gipson et al., 2007). Two palindrome disruption mutations (*tlc1-42G* and *tlc1-42C*) that prevent

291 potential intermolecular base-pairing by this sequence, and the compensatory mutations (*tlc1-*

292 *42G* and *tlc1-42C* in *trans*), which restore the potential for intermolecular base-pairing but not

293 the wild-type palindromic sequence itself, have been described previously (Gipson et al., 2007).

294 We found that the palindrome disruption mutations *tlc1-42G* and *tlc1-42C*, when incorporated

295 into untagged TLC1 in the strains also expressing TLC1-MS2, reduced TLC1-TLC1 coIP by

296 over half (Figure 3C). The compensatory mutations, *tlc1-42G* and *tlc1-42C* in *trans*, although

297 restoring intermolecular base-pairing potential, failed to restore the TLC1-TLC1 coIP level

298 (Figure 3C). The total levels of these mutant telomerase RNAs were unchanged from wild type;

299 hence, efficient *in vivo* association between mature TLC1 molecules requires the specific

300 sequence - and not simply its potential for base pairing *in trans* - of a palindromic motif located

301 in the cleaved-off 3' portion of the TLC1 precursor. These results indicate that at least some

302 TLC1-TLC1 association initiates during telomerase biogenesis before processing produces the

303 mature TLC1 3' end.

304

305 TLC1-TLC1 Association is dependent on nuclear export and is cell cycle-regulated

306 Maturation of telomerase RNA including 3' end processing takes place partially in the cytoplasm

307 (Gallardo et al., 2008). Interestingly, while deletion of Tgs1, which is responsible for TLC1 m3G

308 cap formation (Franke, Gehlen & Ehrenhofer-Murray, 2008), had no effect on total TLC1 levels

309 and little effect on TLC1-TLC1 association (p > 0.05), mutating Nup133 (required for nuclear

310 export) (Gallardo et al., 2008) diminished by at least half the fraction of TLC1 in the associated

311 form, while causing no effect on total TLC1 levels (p < 0.05; Figure 4A). This finding indicated

312 that TLC1 export into the cytoplasm may be necessary for TLC1-TLC1 association.

313 TLC1 maturation by 3' end processing is reported to be active only during G1 phase of the cell

314 cycle (Chapon, Cech & Zaug, 1997). To test whether TLC1-TLC1 association is controlled

315 during the cell cycle, yeast cell lysates were prepared at 15-minute intervals from cells following

316 release into G1 phase from an alpha-factor arrest. Cell cycle progression and synchrony were

317 confirmed by analysis of the various cyclin mRNA levels throughout the time course (Figure

318 4B). Consistent with a previous report (Mozdy & Cech, 2006), the total TLC1 steady-state levels

319 showed a slight increase as the cell cycle progressed (Figure 4C). During the first cell cycle after

320 the release from the 2-hour alpha-factor arrest, the fraction of TLC1 in dimer form in the coIP

321 assay remained relatively constant (Figure 4D). Then after mitosis, as the cell population re-

322 entered the next G1 phase, the fraction of TLC1-TLC1 association abruptly increased 2-fold,

323 with markedly different kinetics compared to the slow and steady accumulation of total

324 TLC1throughout the cell cycle progression (Figure 4D). This finding is consistent with TLC1-

325 TLC1 association occurring during the biogenesis of telomerase complex, a process that has been

326 detected only in G1 phase. The lack of a higher fraction of TLC1 in the dimer form during the

327 G1 phase immediately following the release from the 2-hour alpha-factor arrest is also consistent

328 with TLC1-TLC1 association during a biogenesis step, since in this situation, cells have been

329 held in G1 phase, in the presence of active biogenesis machinery, for 120 minutes prior to the

330 point of release from alpha-factor. We conclude that TLC1-TLC1 association is cell-cycle-

331 controlled and highest in G1.

332 Telomerase holoenzyme formation is not required for TLC1-TLC1 association

333

334 To test whether there are any protein factors that assist in maintaining the TLC1-TLC1

335 association, we treated the immunoprecipitates with trypsin. We found that protease treatment

336 reduced coIP efficiency by ~40% compared with the control (Figure 5A), suggesting a role for

337 protein(s) in initiating, or stabilizing, TLC1-TLC1 association.

338

339   We tested the most likely protein factor candidate, Est2, the telomerase reverse transcriptase core

340   protein. It has been shown that Est2 and TLC1 come together in the cytoplasm, although when in

341   the cell cycle they initiate the interaction is unclear (Teixeira et al., 2002; Gallardo et al., 2008).

342   In *est2Δ* strains, a diminution in TLC1-TLC1 association of about 20 – 25 % was detected,

343   although this measured reduction was not highly significant when compared to the control wild-

344   type *EST2* strain (p > 0.05; Figure 5B). We reasoned that the modest requirement for Est2 in

345   TLC1-TLC1 association might be reflected in TLC1 mutants known to disrupt the core

346   pseudoknot structure required for Est2-TLC1 interaction. Therefore, we disrupted the TLC1

347   pseudoknot by mutating either side of one stem (intra-base-pairing) made up of conserved

348   sequences CS3 and CS4 (*tlc1-20* and *tlc1-21*), and restored the pseudoknot structure by the

349   compensatory mutations (*tlc1-22*) (Lin et al., 2004). CoIP assays showed that the *in vivo* TLC1-

350   TLC1 association was substantially reduced by the pseudoknot-disruptive mutations *tlc1-20* and

351   *tlc1-21* and fully restored by the compensatory mutations, *tlc1-22* (Figure 5C). Thus, efficient

352   TLC1-TLC1 association requires at least this aspect of normal folding of TLC1, although

353   binding to Est2 is largely dispensable.

354

355   Next, we tested two other essential components of the telomerase holoenzyme, Est1 and Est3, for

356   any roles in the *in vivo* TLC1-TLC1 association. Est1-TLC1 interaction is limited to S-phase of

357   the cell cycle, and Est3 interaction with Est2 requires Est1 and hence is also S-phase dependent

358   (Osterhage, Talley & Friedman, 2006). As in the *est2Δ* strain, the *est3Δ* strain showed a modest

359   but not significant (p > 0.05, Figure 5B) reduction in TLC1-TLC1 association. In *est1Δ*, however,

360   the TLC1-TLC1 association was reduced by ~35% (p < 0.05, Figure 5B). While many aspects of

361   Est1 functions in telomere biology remain unclear, roles for Est1 in the recruitment of telomerase

362   to telomeres as well as in telomerase enzymatic activation are well established (Evans &

363   Lundblad, 2002). The TLC1-TLC1 association showed a somewhat greater dependence on Est1

364   than on Est2 and Est3. This raises the possibility that, rather than the telomerase enzymatic

365   activation function of Est1, the telomere recruitment or other function unique to Est1 may play a

366   role in TLC1-TLC1 association.

367

368   Ku and Sir4, but not Telomere Silencing or Tethering to the Nuclear Periphery, Promote the

369   Same Mode of TLC1-TLC1 Association

370

371   To test whether other factors involved in telomerase recruitment to telomeres also affect TLC1-

372   TLC1 association, we first performed the coIP assays in Ku mutant strains. In contrast to the

373   more modest effects of the absence of essential telomerase components Est1, Est2 or Est3, 60 -

374   75% of the TLC1-TLC1 association was consistently lost in *yku70Δ* and *yku80Δ* strains, as well

375   as in *yku80-135i* strains (Figure 5D), which have a small insertion in Ku that specifically

376   abrogates TLC1-Ku interaction, but leaves NHEJ intact (Stellwagen et al., 2003). As previously

377   reported (Mozdy, Podell & Cech, 2008), in all these Ku mutant strains the steady-state level of

378   total TLC1 was reduced by about 25-50% (Figure 5E), and telomeres, while stable, are shorter

379   than in wild-type. Therefore we tested two different mutations (*cdc73Δ*, *ctr9Δ*) that reduce the

380   steady-state level of TLC1 much more than the Ku mutations (Figure 5E). Neither *cdc73Δ* nor

381   *ctr9Δ* caused any decrease in the fraction of dimeric TLC1 (Figure 5D). Furthermore, two

382   mutations known to cause short telomeres (*arf1Δ and tel1Δ*) (Askree et al., 2004), also did not

383   reduce TLC1-TLC1 association (Figure 5D and E). The combined findings above indicate that

384   Ku binding to TLC1 promotes or stabilizes TLC1-TLC1 association, and that neither reduction

385   in TLC1 steady state level nor shorter, stable telomeres is sufficient to impair TLC1-TLC1

386   association.

387

388   The Ku complex is also necessary for telomere silencing (Boulton & Jackson, 1998) and

389   telomere tethering to the nuclear periphery (Taddei et al., 2004). However, by using mutations

390   that affect these processes, we found evidence that it is not because of these functions that Ku

391   plays a role in TLC1-TLC1 association. Specifically, *sir3Δ* (which abrogates telomere silencing)

392   and neither *ctf18Δ* nor *esc1Δ* (which each diminish telomere tethering) (Hiraga, Robertson &

393   Donaldson, 2006) decreased TLC1-TLC1 association levels (Figure 6A). In marked contrast,

394   *sir4Δ* as well as *sir4-42* mutations diminished TLC1-TLC1 association to the same extent as

395   *yku80-135i and sir2Δ to a lesser extent* (Figure 6A). SIR4-42 mutation truncates the C-terminus

396   of Sir4 and fails to recruit silent chromatin factors to telomeres (Kennedy et al., 1995). Sir4 is

397   distinguished from the other telomere silencing Sir proteins Sir2 and Sir3 by its localization on

398   telomeres closer to the distal tip than Sir2 and Sir3, and the Ku complex is reported to interact

399   physically with Sir4 (Tsukamoto, Kato & Ikeda, 1997). Since Ku and Sir4 are localized on

400   telomeres, we tested whether detection of TLC1-TLC1 association in cell extracts by the coIP

401 assay was dependent on DNA. However, DNase treatment of the extracts did not diminish the

402 fraction of TLC1 detected in dimeric form (Figure 6B).

403

404 To test if the Ku complex and Sir4 act in the same pathway for TLC1-TLC1 association, we

405 combined *sir4Δ with yku80Δ* or *yku80-135i* mutations. The double mutants showed no further

406 reduction in the TLC1 dimer fraction compared to single mutants (Figure 6C). We conclude that

407 Ku binding to TLC1 and Sir4 regulates TLC1-TLC1 association through the same pathway,

408 which is independent of telomere silencing or anchoring to the nuclear periphery.

409

410 Ku/Sir4 and the 3'-Cleaved TLC1 Precursor Sequence Promote TLC1-TLC1 association by

411 Different Modes

412

413 To determine the relationship between the roles of Ku/Sir4 and the 3' region of TLC1 in TLC1-

414 TLC1 association, we combined *sir4Δ* or *yku80Δ* mutation with the 3' mutation *tlc1-42G*. In

415 these double mutants (*sir4Δ tlc1-42G* and *yku80Δ tlc1-42G* strains), compared to either each

416 single-mutant strain or the *sir4Δ yku80Δ* double mutant, the TLC1-TLC1 association was further

417 reduced, down to almost to the background control level (Figure 6D). This indicated that the

418 TLC1-TLC1 association that is dependent on the 3' region of TLC1 is at least partially

419 independent of Ku and Sir4, possibly mediated by a different pathway.

420

421 Lack of Evidence for Est2-Est2 Physical Association

422

423 Although, as described above, we did not find evidence that TLC1-TLC1 association was highly

424 dependent on Est2, we tested the possibility that any of the small fraction of TLC1-TLC1

425 association that may be potentially affected by Est2 deletion might be mediated through

426 association of one Est2 molecule with another Est2 molecule. To this end, we performed four

427 different assays in attempts to detect any such physical Est2-Est2 interaction *in vivo*. First, we

428 attempted to detect Est2-Est2 interaction by yeast two-hybrid assay in which Est2 was fused to

429 the Gal4 activation domain and DNA binding domain separately; such assays showed no positive

430 signals for Est2-Est2 interaction. Secondly, we co-expressed Est2-FLAG and Est2-myc and

431 performed co-immunoprecipitation assays; however, no signal indicative of co-

432   immunoprecipitation was detected in the Western blots in these experiments. Thirdly, to

433   overcome the potential issues of the detection limit using Western blotting, we performed coIP

434   experiments using presence of TLC1 as a proxy signal, via qRT-PCR assays as described above.

435   In this approach, we co-expressed wild-type Est2-HA with either wild-type Est2-myc (positive

436   control) or *est2ΔCP*-myc. *est2ΔCP* deletes the Est2 domain that is required for Est2-TLC1

437   interaction (Lin & Blackburn, 2004). Therefore, the presence of an interaction between Est2-HA

438   and *Est2ΔCP*-myc can be ascertained by proxy using the measurement of TLC1 in *est2ΔCP*-myc

439   IP. However, we did not observe any such enrichment of TLC1 in this coIP assay (Figure 7A).

440   Finally, because TLC1 detection by the qRT-PCR assay had high sensitivity, we also performed

441   sequential coIP experiments with strains co-expressing Est2-FLAG and Est2-myc. In this assay,

442   Est2-FLAG was adsorbed onto anti-FLAG gel matrix and subsequently eluted with FLAG

443   peptide, and any Est2-myc present in the elution fraction was immunoprecipitated with anti-myc

444   antibody. The amount of TLC1 was then quantified in this final immunoprecipitate; while the

445   positive control (Est2-FLAG-myc) showed robust enrichment, we found no enrichment of TLC1

446   compared to the negative control (Figure 7B). We conclude that, although the possibility of a

447   weak or transient association between Est2 molecules cannot be ruled out, these negative lines of

448   evidence are consistent with the model that the majority of the TLC1-TLC1 *in vivo* association is

449   independent of an active telomerase enzyme complex.

450
451   DISCUSSION

452

453   Here we have explored the nature of telomerase RNA-RNA associations *in vivo* in *S. cerevisiae*.

454   We report that ~10% of the TLC1 molecules *in vivo* are physically associated with another TLC1

455   molecule. We refer to this as TLC1-TLC1 association for simplicity, although the data do not

456   formally exclude the possibility of higher oligomerization forms. The lack of formation of

457   TLC1-TLC1 association in lysates (the mix experiments) suggest that either TLC1 level is too

458   low in the lysate or there is an active mechanism required for the association. This TLC1-TLC1

459   association increases by two-fold specifically in G1 phase of the cell cycle, and takes place via

460   two distinguishable modes.

461

462 First, mutating a sequence in the 3' region of TLC1 that is cleaved off during the production of

463 the mature form of TLC1 reduced TLC1-TLC1 association by about half. The TLC1-TLC1

464 association of both the mature and the immature TLC1 forms were comparably affected by this

465 3' sequence mutation. This same sequence has previously been implicated in TLC1-TLC1

466 association *in vitro* and its mutation shown to shorten telomeres (Gipson et al., 2007). Our

467 findings thus indicate this 3' sequence-dependent mode of TLC1-TLC1 association occurs *in*

468 *vivo* during telomerase biogenesis. This is further consistent with our findings that TLC1-TLC1

469 association depends on nuclear export to the cytoplasm, where biogenesis of telomerase is

470 reported to occur, and that TLC1-TLC1 association increases in G1 phase, the only time in the

471 cell cycle when TLC1 maturation cleavage is active (Chapon, Cech & Zaug, 1997).

472

473 The second mode of TLC1-TLC1 association requires Ku binding to TLC1; mutations

474 preventing Ku-TLC1 interaction reduced TLC1-TLC1 association by about half. The Ku-

475 associated protein Sir4 was also required for this mode. The Sir and Ku complexes are both

476 important factors in maintaining telomeres; their functions include forming silent chromatin at

477 telomeres and recruiting telomeres to nuclear periphery (Boulton & Jackson, 1998; Taddei et al.,

478 2004). Interestingly however, although Sir4 is part of the silent information regulator Sir

479 complex, TLC1-TLC1 association required neither classic silencing (neither Sir2 nor Sir3 was

480 required), nor Ku-mediated telomere tethering to the nuclear periphery (neither Esc1 nor Ctf18

481 was required).

482

483 The additive genetic disruptions of these two modes of *in vivo* TLC1-TLC1 association - RNA

484 sequence mutations in the 3' region of TLC1 and deletion of the protein factors Ku and Sir4 -

485 have an intriguing parallel to the *in vitro* disruptions of TLC1-TLC1 association in the

486 immunoprecipitate, via either competition with excess oligonucleotides (most sensitive in the 3'

487 region) or protease treatment. Each of these two *in vitro* treatments disrupted only a fraction of

488 the TLC1-TLC1 association. Combining these findings, the simplest interpretation is that these

489 two fractions correspond to or overlap with the TLC1 3' sequence-dependent and the Ku/Sir4

490 dependent association modes respectively.

491

492   Simultaneously mutating both the 3' precursor TLC1 sequence and abrogating Ku-TLC1 binding

493   abolished *in vivo* TLC1-TLC1 association to background levels. The epistasis analyses together

494   indicate that for physical TLC1-TLC1 association, Ku and Sir4 act in the same pathway, which

495   is distinct from the pathway requiring the 3' end sequence of the immature TLC1 RNA. Notably,

496   each of the various kinds of mutations that we report here to impair TLC1-TLC1 association also

497   causes telomeres to be shorter than wild-type (Askree et al., 2004), consistent with TLC1-TLC1

498   association *in vivo* having functional significance.

499

500   Our findings indicate two separable and potentially independent modes of TLC1-TLC1

501   association – the first involving the TLC1 3' region prior to cleavage to the mature form, and a

502   subsequent mode involving Ku/Sir4. We propose a model (Figure 8) by which all TLC1

503   molecules transiently engage in TLC1-TLC1 association during at least two stages in telomerase

504   biogenesis. The first TLC1-TLC1 association mode occurs prior to TLC1 maturation and

505   requires a sequence in the 3'extension of the TLC1 precursor (Figure 8 Mode 1). The lack of

506   compensatory mutation recue of TLC1-TLC1 association suggests the palindromic sequence in

507   the 3' region may be important for a recruitment of a factor or a secondary structure that is

508   important in TLC1-TLC1 association rather than *trans* base-pairing. The TLC1-TLC1

509   association is further stabilized by RNA-RNA or RNA-protein interactions that persist after

510   TLC1 cleavage/maturation, which can be partially disrupted *in vitro* by anti-sense

511   oligonucleotides - particularly those complementary to the 3' region of the mature telomerase

512   RNA. Our findings suggest that multiple regions of TLC1 RNA help stabilize the TLC1-TLC1

513   association, and are consistent with a model of their "unzipping" caused by the addition of

514   competing oligonucleotides.

515

516   The second mode requires Ku complex binding to TLC1 and also depends on Sir4 (Figure 8

517   Mode II). While it is not known when in the biogenesis and maturation of TLC1 Ku (and

518   possibly Ku-bound Sir4) become associated with TLC1, Ku and Sir4 are both thought to

519   function at telomeres, where the vast majority of TLC1 (>95%) is already processed to the

520   mature form (*i.e.* missing the 3' region). Both mature TLC1 and uncleaved precursor TLC1 were

521   found coIP'ed with Est2, albeit with the IP efficiency of the immature form being reduced by

522   about half (Figure 2G). Thus, cleaving off the 3' region of TLC1 is not an obligatory step for

523   TLC1 in order for it to engage in telomerase enzyme complex formation. This is consistent with

524   the lack of interdependence we found between the 3'sequence-mediated association during

525   TLC1 biogenesis and the Ku/Sir-dependent association.

526

527   Interestingly, some of the data presented here cannot easily be reconciled with the data

528   previously reported. Specifically, Gipson *et al* reported that the compensatory mutations in the 3'

529   palindromic sequence (*tlc1-42G* and *tlc1-42C*) dimerized *in vitro* and rescued telomere

530   shortening in *trans*; however, we observed that the *in vivo* TLC1-TLC1 association is not

531   rescued by *trans* compensatory mutations. We observed no *in vitro* TLC1-TLC1 association in

532   lysates (Figure 2E), while Gipson *et al* showed that high concentrations of *in vitro* transcribed

533   TLC1 readily dimerized *in vitro*. These contrasting observations suggest that *in vitro* and *in vivo*

534   TLC1-TLC1 associations may results from different mechanisms. The rescue of telomere length

535   in strains co-expressing both *tlc1-42G* and *tlc1-42C* observed by Gipson et al may have resulted

536   from increased total TLC1 levels compared to strains expressing *tlc1-42G* or *tlc1-42C* alone.

537   Hence, these observations are not directly contradictory; however further studies delineating the

538   importance of *in vivo* TLC1-TLC1 association with telomerase functions should clarify these

539   seemingly contradictory findings.

540

541   Lin and Blackburn reported physical interactions between Est2 molecules by differentially

542   tagging two copies of Est2 in coIP assays. The same strains were used in this study to test for

543   presence of Est2-Est2 interaction by measuring TLC1 levels as a proxy. Surprisingly, in contrast

544   to published results, TLC1 did not coimmunoprecipitate. It is possible that TLC1 only interacts

545   with monomeric Est2, and that dimeric Est2's are inactive.

546

547   Finally, the presence of two independent modes and machineries for TLC1-TLC1 association

548   suggest that such interaction reflects an important aspect of yeast telomere maintenance biology;

549   a conclusion reinforced by the telomere shortening that results from all the mutations that

550   disrupted TLC1-TLC1 association. However, this report leaves open the detailed mechanisms of

551   these novel *in vivo* TLC1-TLC1 physical association modes that we have demonstrated in this

552   study. One speculation is that these RNA-RNA associations may be important for the stability of

553   telomerase RNA as it is shuttled among cytoplasmic and nuclear compartments for various

554 maturation steps; a possible model is that TLC1-TLC1 association assists the RNA in acting as

555 its own chaperone. We can further speculate that this might be an important regulatory step for

556 telomerase activity, as the yeast telomerase holoenzyme shows no physical evidence of

557 oligomerization. For example, a dissociation of TLC1-TLC1 association, which likely requires

558 energy, may act as a switch mechanism for forming a fully competent telomerase holoenzyme.

559 There are also other cell cycle regulated telomerase activation factors such as Est1 and Ku that

560 recruit telomerase complex to the telomere at different stages of cell cycle, and it is of great

561 interest to test how these factors may affect TLC1-TLC1 associations in cell cycle-dependent

562 manner. Further research will be needed to decipher the mechanistic and functional significance

563 of intermolecular interactions among telomerase components.

564

565

566 ACKNOWLEDGEMENTS

567 The authors thank Tracy Chow, Beth Cimini, Kyle Jay, Jue Lin, Imke Listerman, and Dana

568 Smith for critical reading of the manuscript and helpful discussion.

569

570 REFERENCES

571 Alves D., Li H., Codrington R., Orte A., Ren X., Klenerman D., Balasubramanian S. 2008.

572   Single-molecule analysis of human telomerase monomer. *Nat Chem Biol* 4:287–289.

573 Askree SH., Yehuda T., Smolikov S., Gurevich R., Hawk J., Coker C., Krauskopf A., Kupiec

574   M., McEachern MJ. 2004. A genome-wide screen for Saccharomyces cerevisiae deletion

575   mutants that affect telomere length. *Proceedings of the National Academy of Sciences of*

576   *the United States of America* 101:8658–8663.

577 Baker Brachmann C., Davies A., Cost GJ., Caputo E., Li J., Hieter P., Boeke JD. 1998. Designer

578   deletion strains derived from Saccharomyces cerevisiae S288C: A useful set of strains

579   and plasmids for PCR‐mediated gene disruption and other applications. *Yeast* 14:115–

580   132.

581   Beattie TL., Zhou W., Robinson MO., Harrington L. 2001. Functional Multimerization of the

582   Human Telomerase Reverse Transcriptase. *Mol. Cell. Biol.* 21:6151–6160.

583   Boulton SJ., Jackson SP. 1998. Components of the Ku-dependent non-homologous end-joining

584   pathway are involved in telomeric length maintenance and telomeric silencing. *The*

585   *EMBO Journal* 17:1819–1828.

586   Bryan TM., Goodrich KJ., Cech TR. 2003. Tetrahymena Telomerase Is Active as a Monomer.

587   *Molecular Biology of the Cell* 14:4794–4804.

588   Chan A., Boulé J-B., Zakian VA. 2008. Two Pathways Recruit Telomerase to Saccharomyces

589   cerevisiae Telomeres. *PLoS Genet* 4:e1000236.

590   Chapon C., Cech TR., Zaug AJ. 1997. Polyadenylation of telomerase RNA in budding yeast.

591   *RNA (New York, N.Y.)* 3:1337–1351.

592   Evans SK., Lundblad V. 2002. The Est1 Subunit of Saccharomyces cerevisiae Telomerase

593   Makes Multiple Contributions to Telomere Length Maintenance. *Genetics* 162:1101–

594   1115.

595   Fisher TS., Taggart AKP., Zakian VA. 2004. Cell cycle-dependent regulation of yeast telomerase

596   by Ku. *Nat Struct Mol Biol* 11:1198–1205.

597   Franke J., Gehlen J., Ehrenhofer-Murray AE. 2008. Hypermethylation of yeast telomerase RNA

598   by the snRNA and snoRNA methyltransferase Tgs1. *Journal of Cell Science* 121:3553–

599   3560.

600   Gallardo F., Olivier C., Dandjinou AT., Wellinger RJ., Chartrand P. 2008. TLC1 RNA nucleo-

601   cytoplasmic trafficking links telomerase biogenesis to its recruitment to telomeres.

602   *EMBO J* 27:748–757.

603   Gipson CL., Xin Z-T., Danzy SC., Parslow TG., Ly H. 2007. Functional Characterization of
604   Yeast Telomerase RNA Dimerization. *Journal of Biological Chemistry* 282:18857 –
605   18863.

606   Hiraga S., Robertson ED., Donaldson AD. 2006. The Ctf18 RFC-like complex positions yeast
607   telomeres but does not specify their replication time. *EMBO J* 25:1505–1514.

608   Jain D., Cooper JP. 2010. Telomeric strategies: means to an end. *Annual Review of Genetics*
609   44:243–269.

610   Jiang J., Miracco EJ., Hong K., Eckert B., Chan H., Cash DD., Min B., Zhou ZH., Collins K.,
611   Feigon J. 2013. The architecture of Tetrahymena telomerase holoenzyme. *Nature*
612   496:187–192.

613   Kennedy BK., Austriaco Jr. NR., Zhang J., Guarente L. 1995. Mutation in the silencing gene
614   S/R4 can delay aging in S. cerevisiae. *Cell* 80:485–496.

615   de Lange T., Lundblad V., Blackburn E. 2006. *Telomeres, Second Edition*. Cold Spring Harbor
616   Laboratory Press.

617   Lin J., Ly H., Hussain A., Abraham M., Pearl S., Tzfati Y., Parslow TG., Blackburn EH. 2004. A
618   universal telomerase RNA core structure includes structured motifs required for binding
619   the telomerase reverse transcriptase protein. *Proceedings of the National Academy of*
620   *Sciences of the United States of America* 101:14713–14718.

621   Lin J., Blackburn EH. 2004. Nucleolar protein PinX1p regulates telomerase by sequestering its
622   protein catalytic subunit in an inactive complex lacking telomerase RNA. *Genes &*
623   *Development* 18:387 –396.

624   Mozdy AD., Cech TR. 2006. Low abundance of telomerase in yeast: Implications for telomerase
625   haploinsufficiency. *RNA* 12:1721 –1737.

626 Mozdy AD., Podell ER., Cech TR. 2008. Multiple Yeast Genes, Including Paf1 Complex Genes,

627   Affect Telomere Length via Telomerase RNA Abundance. *Mol. Cell. Biol.* 28:4152–

628   4161.

629 Osterhage JL., Talley JM., Friedman KL. 2006. Proteasome-dependent degradation of Est1p

630   regulates the cell cycle-restricted assembly of telomerase in Saccharomyces cerevisiae.

631   *Nat Struct Mol Biol* 13:720–728.

632 Prescott J., Blackburn EH. 1997. Functionally interacting telomerase RNAs in the yeast

633   telomerase complex. *Genes & Development* 11:2790 –2800.

634 Sauerwald A., Sandin S., Cristofari G., Scheres SHW., Lingner J., Rhodes D. 2013. Structure of

635   active dimeric human telomerase. *Nature structural & molecular biology* 20:454–460.

636 Seto AG., Livengood AJ., Tzfati Y., Blackburn EH., Cech TR. 2002. A bulged stem tethers

637   Est1p to telomerase RNA in budding yeast. *Genes & Development* 16:2800 –2812.

638 Shcherbakova DM., Sokolov KA., Zvereva MI., Dontsova OA. 2009. Telomerase from yeast

639   Saccharomyces cerevisiae is active in vitro as a monomer. *Biochemistry (Moscow)*

640   74:749–755.

641 Stellwagen AE., Haimberger ZW., Veatch JR., Gottschling DE. 2003. Ku interacts with

642   telomerase RNA to promote telomere addition at native and broken chromosome ends.

643   *Genes & Development* 17:2384 –2395.

644 Taddei A., Hediger F., Neumann FR., Bauer C., Gasser SM. 2004. Separation of silencing from

645   perinuclear anchoring functions in yeast Ku80, Sir4 and Esc1 proteins. *EMBO J*

646   23:1301–1312.

647 Teixeira MT., Forstemann K., Gasser SM., Lingner J. 2002. Intracellular trafficking of yeast

648   telomerase components. *EMBO Reports* 3:652–659.

649   Tomlin GC., Wixon JL., Bolotin-Fukuhara M., Oliver SG. 2001. A new family of yeast vectors

650   and S288C-derived strains for the systematic analysis of gene function. *Yeast*

651   *(Chichester, England)* 18:563–575.

652   Tsukamoto Y., Kato J., Ikeda H. 1997. Silencing factors participate in DNA repair and

653   recombination in Saccharomyces cerevisiae. *Nature* 388:900–903.

654   Wang L., Dean SR., Shippen DE. 2002. Oligomerization of the telomerase reverse transcriptase

655   from Euplotes crassus. *Nucleic Acids Research* 30:4032–4039.

656   Wenz C., Enenkel B., Amacker M., Kelleher C., Damm K., Lingner J. 2001. Human telomerase

657   contains two cooperating telomerase RNA molecules. *The EMBO Journal* 20:3526–3534.

658   Zappulla DC., Cech TR. 2004. Yeast telomerase RNA: A flexible scaffold for protein subunits.

659   *Proceedings of the National Academy of Sciences of the United States of America*

660   101:10024 –10029.

661

Strains used

All strains are in the S288c strain background and are isogenic to BY4746 (Tomlin et al., 2001) , except as noted below. BAR1 gene was deleted from BY4720 strain and mated to BY4741 (Baker Brachmann et al., 1998) . The resulting diploid strain became the parental strain for two independent spores, yEHB22,321/465 and yEHB22,322/466. The strains yEHB22,803/804 were generous gift of Jonathan Weissman. All haploid strains have independently isolated isogenic duplicates from parental strains as noted in the table below (denoted by yEHB22,XXX/YYY, which refers to two stains yEHB22,XXX and yEHB22,YYY). The diploid strains, yEHB22,825-827 were created by mating yEHB321/465 and yEHB22,322/466 strains that have Est2 fused to indicated tags. Strains that were further modified in this study are in bold.

1 Table 1. Strains used.

3 All strains are in the S288c strain background and are isogenic to BY4746 (Tomlin et al., 2001),
4 except as noted below. BAR1 gene was deleted from BY4720 strain and mated to BY4741
5 (Baker Brachmann et al., 1998). The resulting diploid strain became the parental strain for two
6 independent spores, yEHB22,321/465 and yEHB22,322/466. The strains yEHB22,803/804 were
7 generous gift of Jonathan Weissman. All haploid strains have independently isolated isogenic
8 duplicates from parental strains as noted in the table below (denoted by yEHB22,XXX/YYY,
9 which refers to two stains yEHB22,XXX and yEHB22,YYY). The diploid strains, yEHB22,825-
10 827 were created by mating yEHB321/465 and yEHB22,322/466 strains that have Est2 fused to
11 indicated tags. Strains that were further modified in this study are in bold.

Strain number	Relevant genotype
yEHB22,321/465	***ADE2 his3Δ1 leu2Δ0 lys2Δ0 met15Δ0 trp1Δ63 ura3Δ0 bar1Δ0 MATa***
yEHB22,322/466	***ADE2 his3Δ1 leu2Δ0 lys2Δ0 met15Δ0 trp1Δ63 ura3Δ0 bar1Δ0 MATα***
yEHB22,495/496	yEHB22,321/465 but *TLC1-MS2*
yEHB22,720/721	**yEHB22,321/465 but *HIS3-P$_{CYC1}$-CP-3xMyc***
yEHB22,722/723	yEHB22,720/721 but *TLC1-MS2*
yEHB22,662/663	**yEHB22,720/721 but *TLC1-URA3-TLC1-MS2***
yEHB22,750/751	**yEHB22,720/721 but *TLC1-LEU2-TLC1-MS2***
yEHB22,742/743	yEHB22,720/721 but *tlc1-42G-URA3-TLC1-MS2*
yEHB22,744/745	yEHB22,720/721 but *tlc1-42C-URA3-TLC1-MS2*
yEHB22,776/777	yEHB22,720/721 but *tlc1-42C-URA3-tlc1-42G-MS2*
yEHB22,704/705	yEHB22,662/663 but *tgs1Δ::KanMX6*
yEHB22,768/769	yEHB22,750/751 but *nup133Δ::KanMX6*
yEHB22,698/699	yEHB22,662/663 but *est1Δ::KanMX6*
yEHB22,724/725	yEHB22,662/663 but *est2Δ::KanMX6*
yEHB22,700/701	yEHB22,662/663 but *est3Δ::KanMX6*
yEHB22,682/683	yEHB22,662/663 but *yku70Δ::KanMX6*
yEHB22,686/687	yEHB22,662/663 but *yku80Δ::KanMX6*
yEHB22,758/759	yEHB22,750/751 but *yku80-135i*
yEHB22,702/703	yEHB22,662/663 but *arf1Δ::KanMX6*
yEHB22,706/707	yEHB22,662/663 but *cdc73Δ::KanMX6*
yEHB22,726/727	yEHB22,662/663 but *ctr9Δ::KanMX6*
yEHB22,764/765	yEHB22,750/751 but *ctf18Δ::KanMX6*
yEHB22,766/767	yEHB22,750/751 but *esc1Δ::KanMX6*
yEHB22,728/729	yEHB22,662/663 but *sir2Δ::KanMX6*
yEHB22,762/763	yEHB22,750/751 but *sir3Δ::KanMX6*
yEHB22,730/731	yEHB22,662/663 but *sir4Δ::KanMX6*
yEHB22,787/788	yEHB22,662/663 but *sir4-42::KanMX6*
yEHB22,770/771	yEHB22,750/751 but *tel1Δ::KanMX6*
yEHB22,774/775	yEHB22,662/663 but *sir4Δ::KanMX6 yku80Δ::TRP1*
yEHB22,776/777	yEHB22,720/721 but *tlc1-42G-URA3-TLC1-MS2 yku80Δ::TRP1*
yEHB22,803/804	***LYS2 can1Δ::STE2$_P$-HIS5 lyp1Δ::STE3$_P$-LEU2 MATα***

yEHB22,805/806	yEHB22,803/804 but *TLC1-MS2*
yEHB22,807/808	**yEHB22,803/804 but *TLC1-URA3-TLC1-MS2***
yEHB22,809/810	yEHB22,803/804 but *tlc1-42G-URA3-TLC1-MS2*
yEHB22,811/812	yEHB22,803/804 but *tlc1-42C-URA3-TLC1-MS2*
yEHB22,813/814	yEHB22,803/804 but *tlc1-42C-URA3-tlc1-42G-MS2*
yEHB22,815/816	yEHB22,807/808 but *yku80-135i*
yEHB22,817/818	yEHB22,807/808 but *sir4Δ::KanMX6*
yEHB22,819/820	yEHB22,807/808 but *sir2Δ::KanMX6*
yEHB22,821/822	yEHB22,807/808 but *sir4Δ::KanMX6 yku80-135i*
yEHB22,823/824	yEHB22,803/804 but *tlc1-42G-URA3-TLC1-MS2 sir4Δ::KanMX6*
yEHB22,825	*EST2-3xFLAG/EST2-13xMyc MATa/α*
yEHB22,826	*EST2-3xFLAG/EST2 MATa/α*
yEHB22,827	*EST2-3xFLAG-13xMyc/EST2 MATa/α*

Primer sequences for qRT-PCR

1 Table 2. Primer sequences for qRT-PCR

Amplicon	Primer number	Sequence (5' to 3')
PGK1	oEHB22,0716	GGCTGGTGCTGAAATCGTTCCAAA
	oEHB22,0717*	AGCCAGCTGGAATACCTTCCTTGT
Untagged *TLC1*	oEHB22,0561	CATCGAACGATGTGACAGAGAA
	oEHB22,0801*	GACAAAAATACCGTATTGATCATTAA
MS2-tagged *TLC1*	oEHB22,0563	ATGCCTGCAGGTCGACTCTAGAAA
	oEHB22,0338*	TGCGACAAAAATACCGTATTGATCA
Uncleaved, untagged *TLC1*	oEHB22,1015	TATCTATTAAAACTACTTTGATGATCAGTA
	oEHB22,1038*	AGCGATATACAAGTACAGTACGCGCG
Uncleaved, MS2-tagged *TLC1*	oEHB22,0339	AGCTTGCATGCCTGCAGGTCGACTC
	oEHB22,1038*	AGCGATATACAAGTACAGTACGCGCG
CLN2	oEHB22,712	TTGTTCGAGCTGTCTGTGGTCACT
	oEHB22,713*	AATTTGGCTTGGTCCCGTAACACG
CLN3	oEHB22,837	AAGGCCGCTGTACAACCTGACTAA
	oEHB22,838*	TGAACCGCGAGGAATACTTGTCCA

4   *Primer used in the reverse transcription step

TLC1-TLC1 features and MS2 hairpin insertion

1A. Schematic and linear maps of relevant features of TLC1 RNA coding sequence before it is polyadenylated and cleaved (+1-1301). TmG: 5' trimethylG cap ((Franke, Gehlen & Ehrenhofer-Murray, 2008)); The binding sites for Ku (+288-335), Est1 (+660-664), and Sm (+1153-1160) proteins are indicated. Telomeric template: (+468-484); CS3 (+719-784) and CS4 (+785-853): two sequences, conserved in budding yeasts, that form two sides of a stem of the evolutionarily conserved telomerase RNA pseuduoknot structure ((Lin et al., 2004)); MS2: site of the tandem inserted MS2 coat protein-binding hairpins used in this work, at BclI site (+1033); cleavage site: the 3' end of the mature TLC1 (+1167); CGCGCG: sequence (+1204) previously implicated in TLC1 *in vitro* dimerization, located in the cleaved-off 3' extension of pre-processed immature TLC1 RNA ((Chapon, Cech & Zaug, 1997)). 1B. Anti-sense oligonucleotides targeted against the full length of TLC1. Each of the 72 anti-sense oligonucleotides are 30 bases in length and overlap with each other by 2-5 bases. The oligos are divided into 9 groups (alternating set of blue and red) of 8 oligos. 1C. The MS2 RNA binding hairpins were inserted at NcoI (nucleotide position 455) or BclI (nucleotide position 1033) of TLC1 RNA coding gene. The telomere Southern blot of Y' telomeres shows the impact of the MS2 insert at different positions. The table at the top denotes where the MS2 was inserted (at either nucleotide positions 455 or 1033). F and R denote whether the MS2 hairpin was inserted in correct (F) or in reverse (R) direction. The MS2 insertion at 1033 position seem to have the least impact on the telomere length (yEHB22,495/496). WT = yEHB22,321/465.

A.

B.

C.
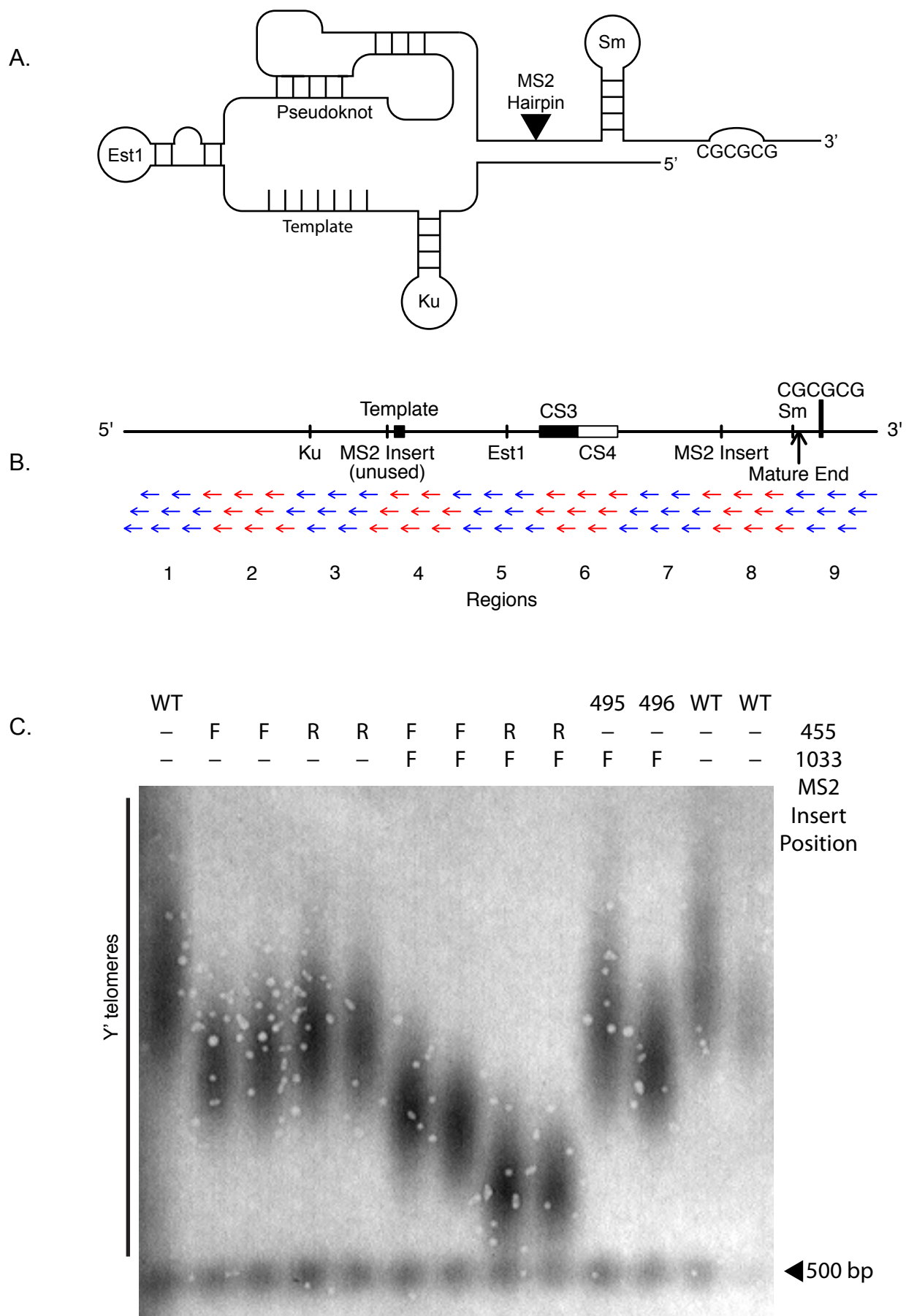
Detection of TLC1-TLC1 Association

2A. Primers used for specifically quantifying untagged or MS2-tagged TLC1 by qRT-PCR is shown schematically. The sequences of these primers are presented in Table 2. The bulge represent the MS2 sequence inserted at the BclI site of TLC1. The forward primer for specifically quantifying untagged TLC1 spans the insertion site of MS2. 2B. The amounts of untagged or MS2-tagged TLC1 were quantified in strains expressing only untagged TLC1 (yEHB22,321/465) or only MS2-tagged TLC1 (yEHB22,495/496). The lysates were also mixed 1:1 in the last two groups (yEHB22,321+yEHB22,495 and yEHB22,465+yEHB22,496). PGK1 values were normalized to the average of all samples. Untagged and MS2-tagged TLC1 values were normalized to the averages of yEHB22,321/465 and yEHB22,495/496, respectively. The error bars indicate the standard deviation of technical triplicates. The numbers below the x-axis represent the "yEHB22,xxx" strains, and the table below indicates the presence of untagged or MS2-tagged TLC1 in each sample. 2C. The amounts of untagged and MS2-tagged TLC1 in total RNA normalized to PGK1 mRNA level are shown. TLC1 was expressed from the genomic locus (yEHB22,662/663) or on a CEN-ARS plasmid (pRS416-TLC1 in yEHB22,722/723). MS2-tagged TLC1 were expressed from the genomic locus. In "Mix" samples, two strains expressing tagged (yEHB22,722/723) and untagged TLC1 (yEHB22,720/721) independently were mixed before the lysis step. The error bars indicate standard deviation from two experiments. 2D. The MS2 -tagged TLC1 associated with Est2. The fraction of tagged and untagged TLC1 coimmunoprecipitated with Myc tagged Est2 was quantified and normalized to the untagged TLC1 fraction. The lysates from yEHB22,321/465 strains carrying pRS426-EST2-Myc was used. The error bar indicates the standard deviation between two experiments. 2E. Detection of TLC1-TLC1 association by the co-immunoprecipitation strategy. The amount of untagged TLC1 co-immunoprecipitated with MS2-tagged TLC1 was used to estimate the fraction of total TLC1 that is dimeric. The calculation method is described in the Methods. Lysates from strains carrying untagged and

MS2-tagged TLC1 were used (WT = yEHB22,662/663). As negative controls, separate strains carrying either MS2-tagged or untagged TLC1 (MS2-tagged = yEHB22,722/723, yEHB22,805/806, untagged = yEHB22,720/721) were mixed just before lysis. The error bars indicate the standard errors among the experiments, and the numbers just below the x-axis denote the number of experiments performed. 2F. The immature TLC1 molecules accounts for only 4-8% of the total level of TLC1 molecules, and that this fraction was unchanged in the co-immunoprecipitated versus total TLC1. The lysates from the strains yEHB22,662/663 were used. The immature TLC1 quantity was divided by the total TLC1 amount, and the ratio was normalized to the input ratio. The error bars indicate standard deviation between two experiments. 2G. The immature TLC1 associated with Est2. The fraction of TLC1, total or immature, coimmunoprecipitated with FLAG-tagged Est2 was quantified and normalized to the total TLC1 fraction. The lysates from yEHB22,826. The error bar indicates the standard deviation between two experiments.
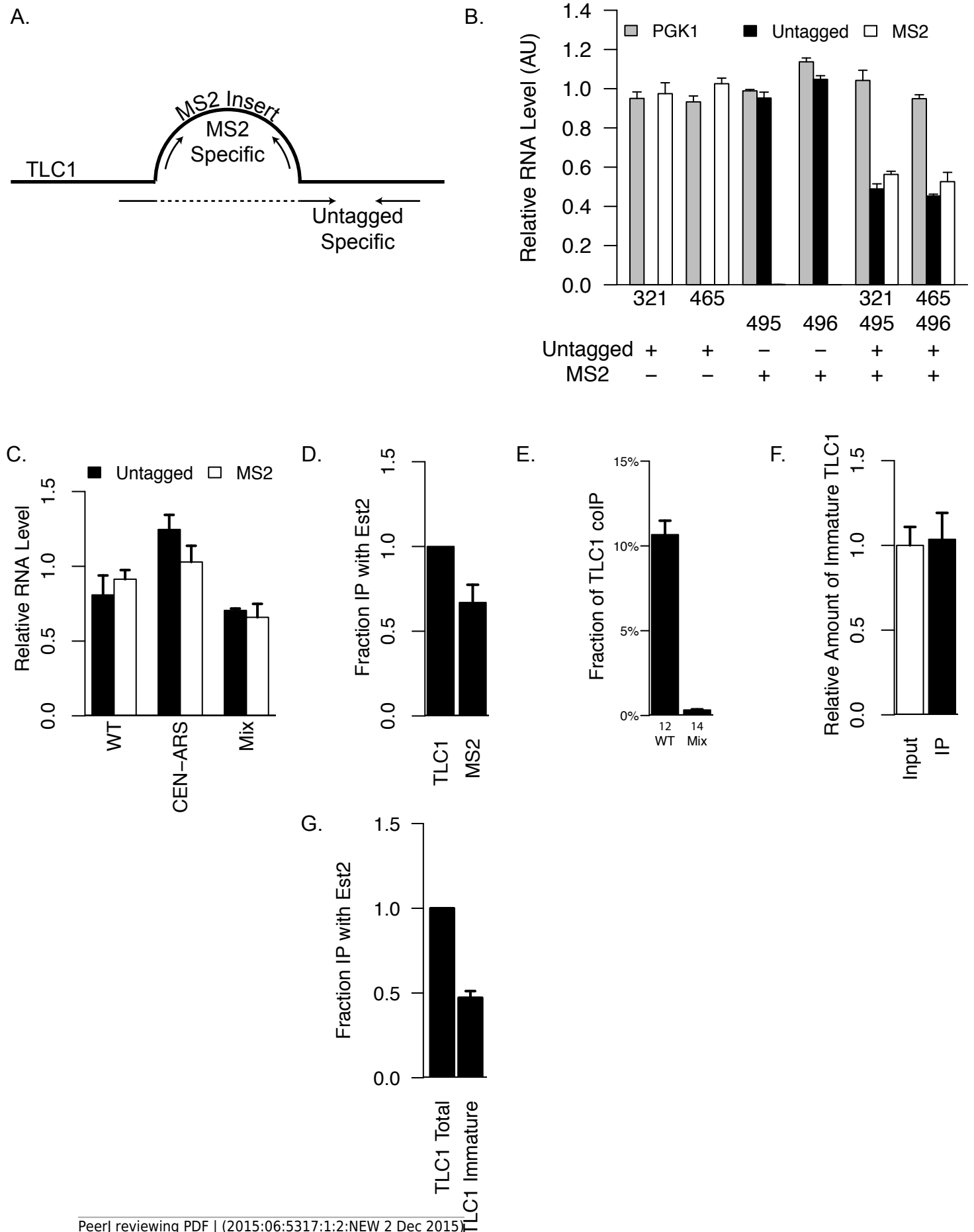
Regions of TLC1 involved in TLC1-TLC1association

3A. Anti-sense oligonucleotides can disrupt TLC1-TLC1association. Anti-sense
oligonucleotides were designed against *TLC1* and incubated with the MS2
immunoprecipitates. The lysates from yEHB22,807/808 were used for these experiments. The
fraction of untagged TLC1 that remained on the beads with the MS2-tagged TLC1 compared
to the average of the sample that had no oligonucleotides or random oligonucleotides added
is shown. All 72 anti-*TLC1* primers or 72 random primers were added. The error bars indicate
the standard errors between the two experiments. 3B. Different subsets of oligonucleotides
were added during the wash step of immunoprecipitation. The lysates from yEHB22,807/808
were used for these experiments. Each box represents the TLC1 region against which
oligonucleotides added targeted. Each ninth and third region contained 8 and 24
oligonucleotides respectively. Shown in each box is the fraction of TLC1 that remained on the
beads after the competition assay compared to the average of the sample that had no
oligonucleotides or random oligonucleotides added (standard deviation in parentheses). 3C.
The TLC1 3' region that is cleaved off plays a role in TLC1 dimerization. The fractions of TLC1
in dimer form, normalized to WT, are shown for strains that carry mutations that disrupt
palindromic sequence in the 3' region of TLC1. WT=CGCGCG (yEHB22,662/663,
yEHB22,807/808), 42G=CGGGGG (yEHB22,742/743, yEHB22,809/810), 42C=CCCCCG
(yEHB22,744/745, yEHB22,811/812), 42G+C=CGGGGG+CCCCCG (yEHB22,776/777,
yEHB22,813/814). The error bars indicate the standard errors among the samples. The
numbers of experiments represented are shown just below the x-axis.

Figure 3
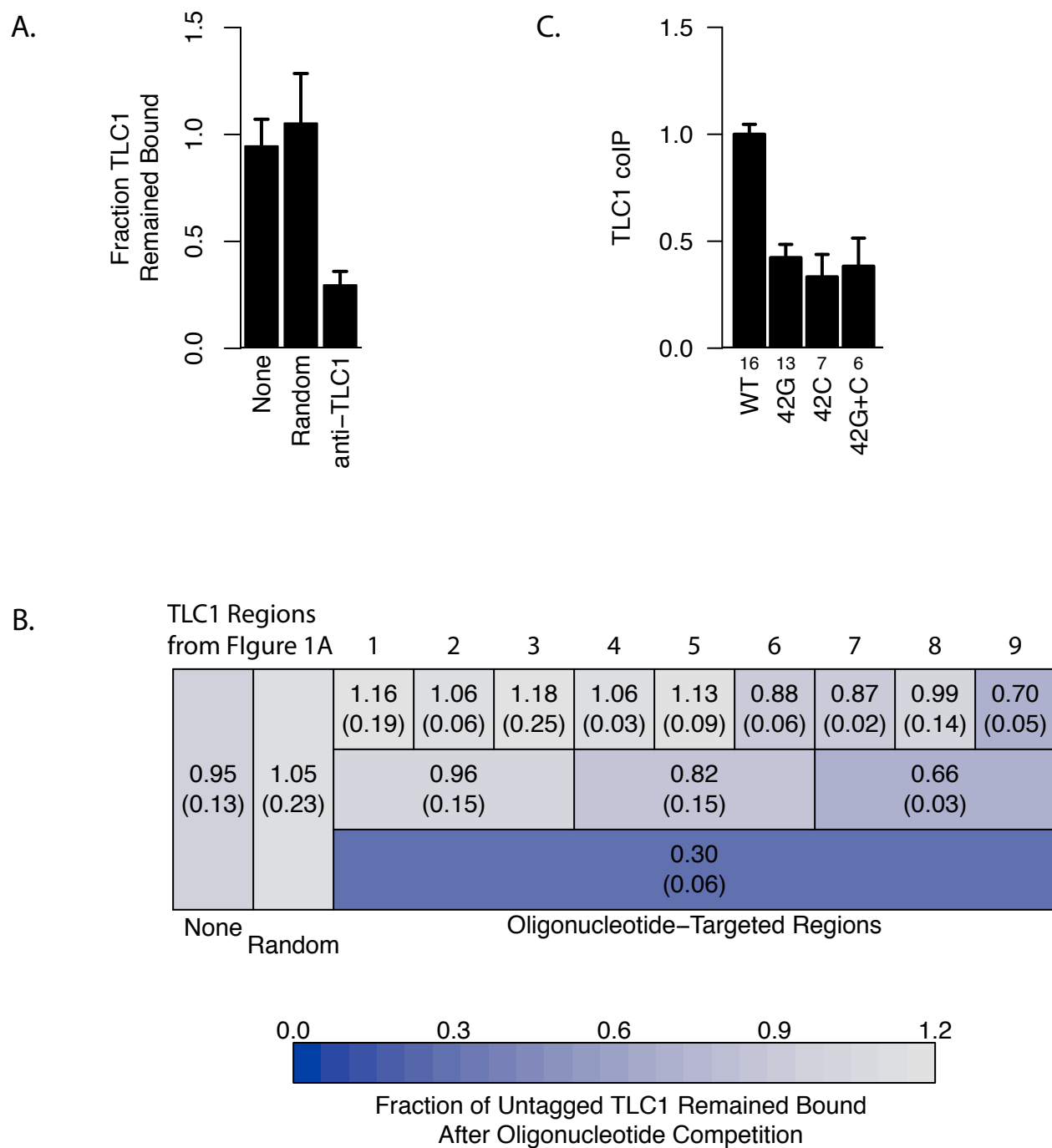
TLC1-TLC1 Association and TLC1 Biogenesis

4A. TLC1 transport to the cytoplasm is required for TLC1-TLC1 association The fractions of TLC1 in dimer form, normalized to WT, are shown for strains that have indicated genes involved in TLC1 biogenesis pathway is deleted. WT = yEHB22,662/663, tgsΔ = yEHB22,704/705, nup133D = yEHB22,768/769. The error bars represent standard errors among the samples, and the numbers of experiments represented are shown just below the x-axis. The asterisk denotes p < 0.05. 4B. Cells (yEHB22,662/663) were arrested in alpha-factor, released and collected every 15 minutes. The first sample (t=0 min) is from alpha-factor arrested cells. Levels of cyclin mRNAs measured to track cell-cycle progress. The values are normalized so that the lowest value is 0 and the highest value is 1. The horizontal bars show cell cycle phase ascertained from the measured cyclin mRNA expression levels shown. 4C. Total TLC1 levels, tagged and untagged, are shown, normalized to the asynchronous culture. The error bars indicate standard deviation between two experiments. 4D The fraction of TLC1 in dimer form calculated from coIP experiments are shown. The values are normalized to the asynchronous sample, and the error bars represent the standard deviation between two experiments.

Figure 4
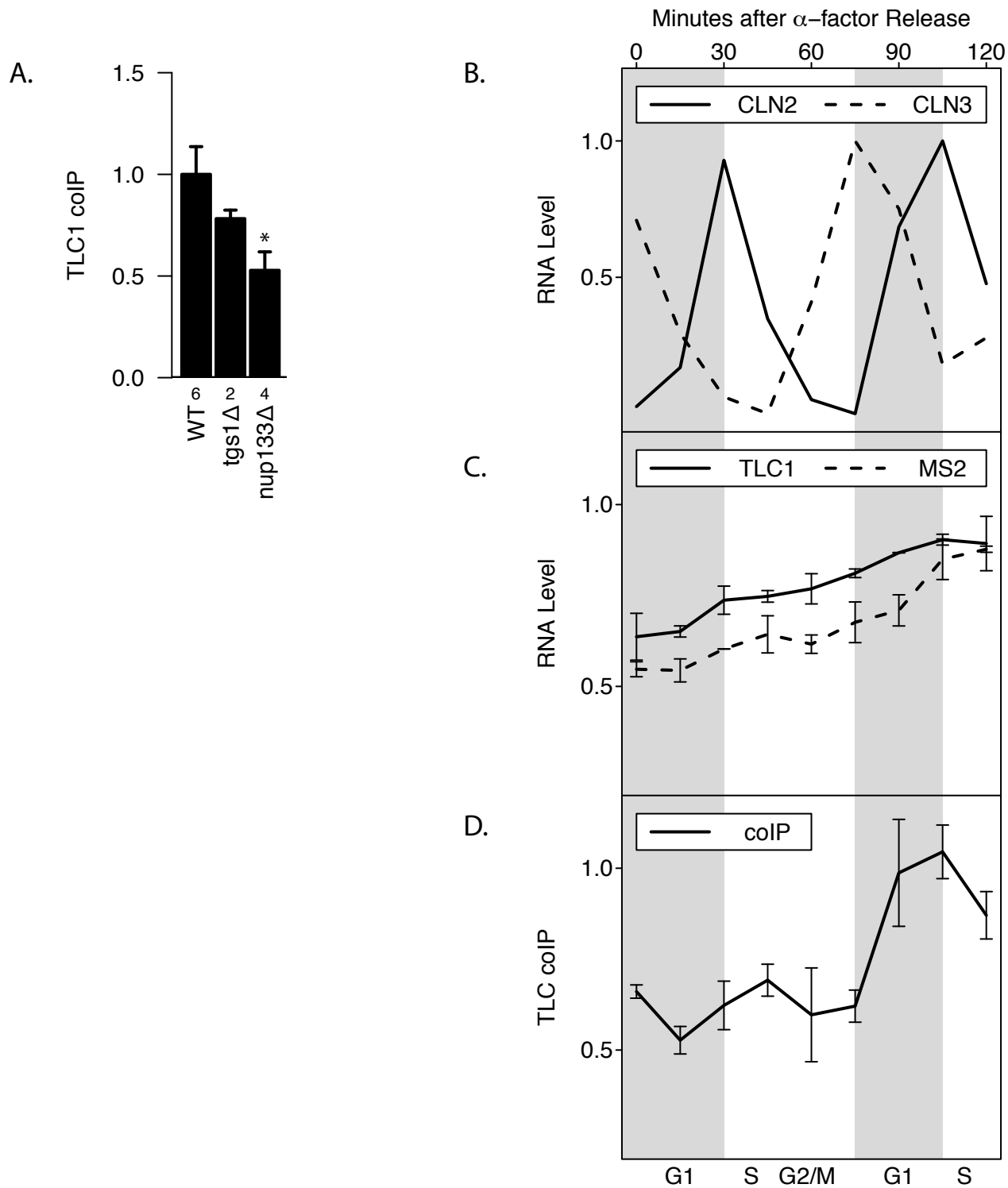
Protein factor requirements for TLC1-TLC1 association

5A. TLC1 dimerization is partially sensitive to trypsin treatment. The fraction of TLC1 that remained in the dimer form after mock or trypsin treatment was measured in lysates from WT strains (yEHB22,807/808). The values were normalized to the average of trypsin-untreated samples. The error bars indicate the standard error between two experiments. The numbers of experiments represented are shown just below the x-axis. 5B. TLC1 dimerization is only modestly affected by absence of Est 1, 2 or 3. The fractions of TLC1 in dimer form, normalized to WT, are shown for strains that have indicated gene is deleted. WT = yEHB22,662/663, est1Δ = yEHB22,698/699, est2Δ = yEHB22,724/725, est3D = yEHB22,700/701. The error bars represent the standard deviation between samples. The numbers of experiments represented are shown just below the x-axis. The asterisk denotes p < 0.05. 5C. Est2 interactions with TLC1 affect TLC1-TLC1 associations. The RNA pseudoknot structure critical for Est2 binding to TLC1 was mutated (cs3 and cs4) and compensatory mutation (cs3-cs4) was introduced. The fractions of TLC1 in dimer form, normalized to WT, are shown for strains carrying these tlc1 mutations. The strains yEHB22,722/723 carrying CEN-ARS plasmids were used: WT = pRS316-TLC1, cs3 = pRS316-tlc1-21, cs4 = pRS316-tlc1-20, cs3-cs4 = pRS316-tcl1-22. These plasmids were generous gift from Jue Lin (Lin et al., 2004) . The error bars indicate the standard error, and the numbers of experiments represented are shown just below the x-axis. 5D TLC1 dimerization requires Ku. The fractions of TLC1 in dimer form, normalized to WT, are shown for strains mutated for indicated genes. WT = yEHB22,662/663, yEHB22,750/751, yEHB22,807/808, yku70D = yEHB22,682/683, yku80Δ = yEHB22,662/663, yku80-135i = yEHB22,750/751, yEHB22,815/816, tel1Δ = yEHB22,770/771, arf1Δ = yEHB22,702/703, cdc73D = yEHB22,706/707, ctr9Δ = yEHB22,727. The error bars indicate the standard error among the samples, except for *ctr9Δ* sample, which was done only once. The numbers of experiments represented are shown just below the x-axis. 5E. Total TLC1 levels do not determine the fraction of TLC1 in the dimer form.

Untagged TLC1 levels in the total RNA were measured in strains deleted for the indicated genes. The levels were normalized to PGK1 mRNA levels first and then to the wild-type levels. The error bars indicate the standard error among the samples, except for *ctr9Δ* sample, which was done only once. The strains used are the same as noted in Figure 4D. The numbers of experiments represented are shown just below the x-axis.
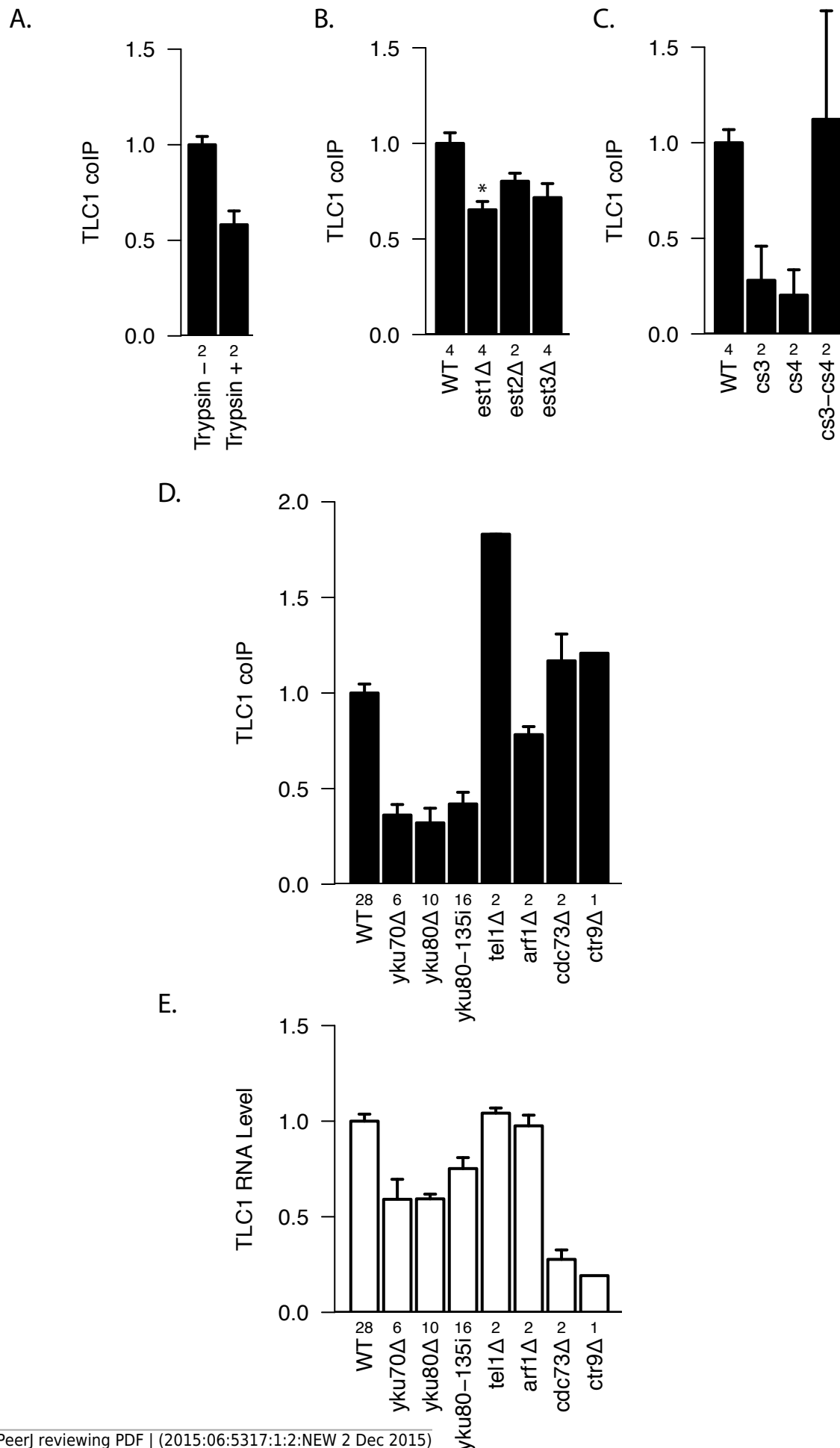
Two separate pathways of TLC1-TLC1 association

6A. Ku complex binding to TLC1 and Sir4 are required for TLC1-TLC1 association but telomere tethering to the nuclear periphery and telomere silencing are not. Mutations defective in either telomere tethering to nuclear periphery (*ctf18Δ* = yEHB22,764/765, and *esc1D* = yEHB22,766/767) or telomere silencing (*sir2Δ* = yEHB22,728/729, yEHB22,819/820, *sir3D* = yEHB22,762/763, *sir4Δ* = yEHB22,730/731, yEHB22,817/818, and *sir4-42* = yEHB22,787/788) are indicated. The fractions of TLC1 in dimer form, normalized to WT (yEHB22,662/663, yEHB22,807/808), are shown for strains indicated. The error bars indicate the standard error, and the numbers of experiments represented are shown just below the x-axis. 6B. Lysate was either untreated, mock-treated, or treated with DNase prior to immunoprecipitation. The efficient loss of DNA was validated only in DNase treated samples. Despite the loss of DNA in the samples, the TLC1-TLC1 coIP efficiency was not reduced. WT strains (yEHB22,662/663) were used for "Coex" samples. In "Mix" samples, strains expressing tagged and untagged TLC1 independently (yEHB22,720/721 and yEHB22,722/723) were mixed before the lysis step. The fraction of TLC1 in dimer form, normalized to the average of "Coex" samples are shown. The error bars indicate the standard error, and the numbers of experiments represented are shown just below the x-axis. 6C. The Ku mutations were combined with *SIR4* deletion. The values are normalized to the average of the wild-type samples in each experiment. The error bars indicate the standard deviation among the samples. The fractions of TLC1 in dimer form, normalized to WT, are shown for strains indicated. WT = yEHB22,662/663, yEHB22,807/808, sir4Δ = yEHB22,730/731, yEHB22,817/818, yku80-135i = yEHB22,750/751, yEHB22,815/816, yku80-135i sir4Δ = yEHB22,821/822, yku80D = yEHB22,662/663, yku80Δ sir4Δ = yEHB22,774/775. The error bars indicate the standard error, and the numbers of experiments represented are shown just below the x-axis. 6D. The Ku and Sir4 combined with the mutation in the 3' region. The deletion strains for *SIR4* and *YKU80* were combined with *tlc1-42G* (42G) mutations. The fractions of TLC1 in dimer form,

normalized to WT, are shown for strains indicated. WT = yEHB22,662/663, yEHB22,807/808, 42G = yEHB22,742/743, yEHB22,809/180, sir4Δ = yEHB22,730/731, yEHB22,817/818, sir4D 42G = yEHB22,823/284, yku80Δ = yEHB22,662/663, yku80Δ 42G = yEHB22,776/777. The error bars indicate the standard error, and the numbers of experiments represented are shown just below the x-axis.

Figure 6
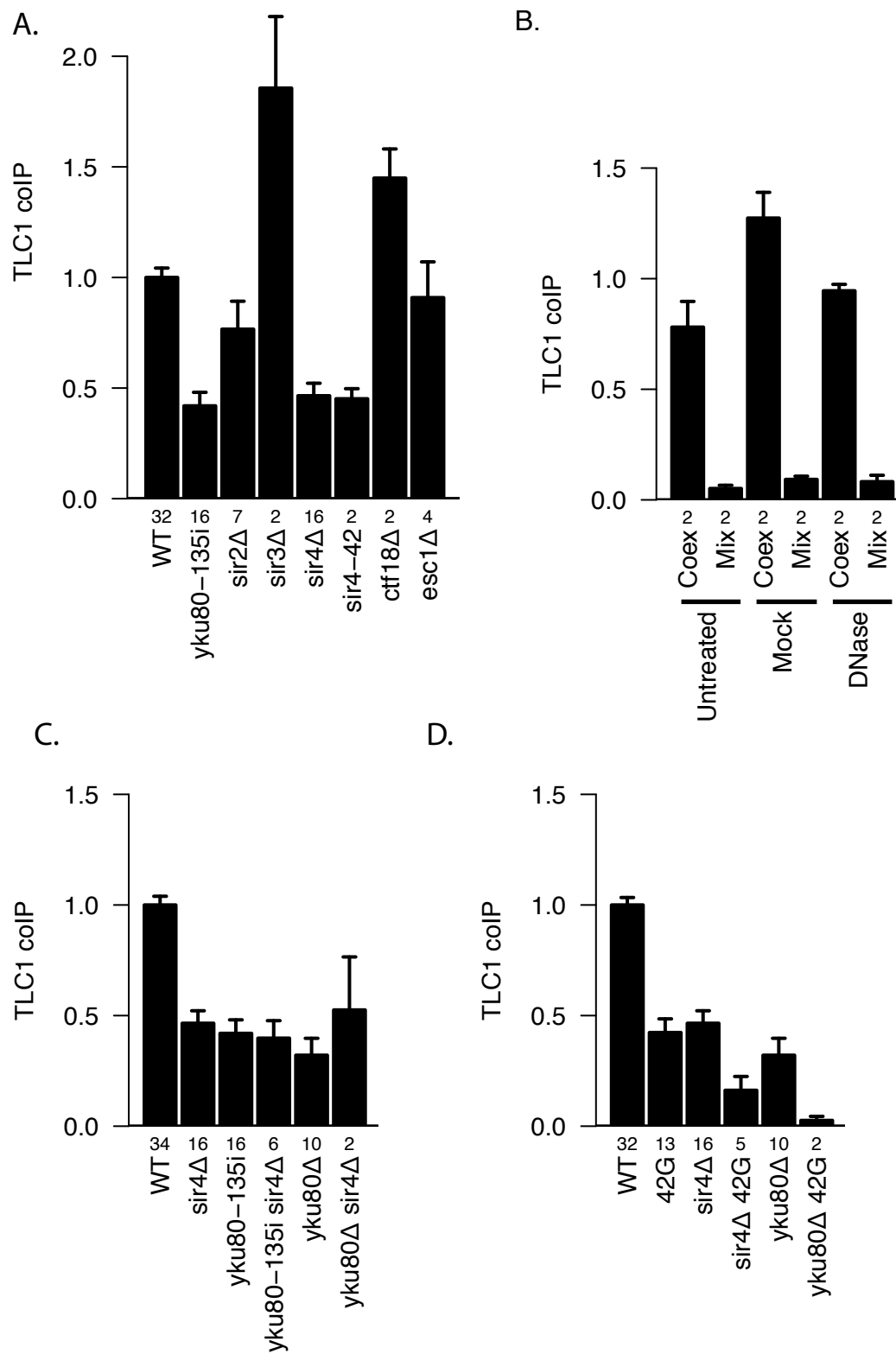
Lack of Evidence for Est2-Est2 association *in vivo*

7A. Est2-ΔCP lacks the Est2 TLC1 binding domain. Myc-tagged Est2 (either Est2-Myc or Est2-ΔCP) was immunoprecipitated from lysates of strains co-expressing Est2-HA. Fractions of TLC1 isolated are shown. Error bars represent standard deviation from two experiments. The table below identify whether CP region of Est2 is deleted (Δ) in Myc or HA-tagged Est2. The strains used in these experiments were generous gift of Jue Lin (Lin & Blackburn, 2004) . 7B. The amount of TLC1 immunoprecipitated after sequential immunoprecipitation, anti-FLAG then anti-MYC, was measured. Amount of TLC1 remained in the MYC IP is represented as the fraction of TLC1 immunoprecipitated in the FLAG IP. The table below indicates EST2 fusions with specified tags present in each IP. The strains yEHB22,825-827 were used in these experiments.
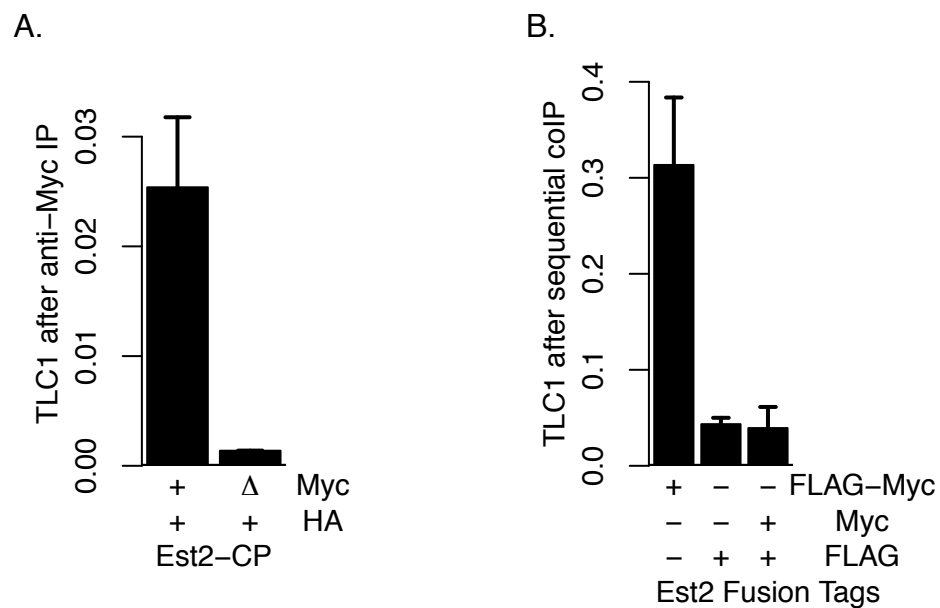
Two modes of dimerization model

Top: Schematic of TLC1 cleavage of 3' region. Tick marks: template region of TLC1. CGCGCG: sequence at the 3' region important in TLC1 dimerization. The stem-loop structure that the Ku complex binds is indicated. (Middle) Two modes of TLC1-TLC1 association in vivo. Mode I, dependent on the precursor TLC1 3' region, is initiated before the 3' region is cleaved off. Mode II, dependent on Sir4/2 and the Ku complex, possibly at telomeres. TLC1 in the telomerase RNP is either monomeric or dimeric, but each RNP contains only one Est2 (bottom).

Maturation
3' cleavage

G1 phase

Ku-binding arm

Dimerization Modes

3' region-dependent

Ku- and Sir4/2-dependent

Unknown factor or
secondary structure

CGCGCG

CGCGCG

AAA

AAA

Ku

Sir4

Sir2

Ku

Sir4

Sir2

?

Mode I: 3' region

Mode II: Ku-mediated

Single Reverse Transcriptase (Est2)

Est2

OR

+ one copy of TLC1

+ two copies of TLC1